QUARTERLY TECHNICAL PROGRESS REPORT
FOR THE PERIOD ENDING SEPTEMBER 30, 2006

TITLE: ANALYSIS OF CRITICAL PERMEABLITY, CAPILLARY PRESSURE AND ELECTRICAL PROPERTIES FOR MESAVERDE TIGHT GAS SANDSTONES FROM WESTERN U.S. BASINS

DOE Contract No. DE-FC26-05NT42660

Contractor: University of Kansas Center for Research, Inc.
2385 Irving Hill Road
Lawrence, KS 66044

DOE Program: Natural Gas Technologies (Advanced Diagnostics & Imaging)

Award Date: October 1, 2005

Total Project Budget: $513,834

DOE Cost Amount: $411,030

Program Period: October 1, 2005 – September 30, 2007

Reporting Period: July 1, 2006 – September 30, 2006

DOE Project Manager: Gary Sames, NETL Morgantown, PN

Contractor Contact: Alan P. Byrnes
Kansas Geological Survey
1930 Constant Ave., Lawrence, Kansas 66047
email: abyrnes@kgs.ku.edu
phone: 785-864-2177

Principal Investigators: Alan P. Byrnes (Program Manager)
Robert Cluff (Discovery Group)
John Webb (Discovery group)

DISCLAIMER:

ABSTRACT:

Analysis of the remaining core plugs of the total of approximately 1300 unique sample depths and 700 duplicate core plugs has been proceeding. Arrangements have been made for obtaining final additional samples from industry participants in the next quarter. Analysis of the basic petrophysical properties of the Mesaverde cores measured-to-date indicates that the samples obtained for each basin exhibit approximately the entire porosity and permeability range exhibited by the Mesaverde for all samples analyzed. Grain density for all samples averages 2.654$\pm$0.033 g/cc (error of 1 std dev) with grain density distributions differing slightly among basins. Analysis of the permeability data indicates that the Klinkenberg gas slip proportionality constant, b, can be predicted using the relation: $b(atm) = 0.851\ k_{ik}^{-0.341}$. This equation is similar to previously reported equations but extends previous work to lower permeability and significantly increases the population for permeabilities less than 0.01 mD. Using multivariate linear regression analysis the relationship between *in situ* porosity (ϕ_i), the rock characterization size-sorting digit 2 (RC2) and *in situ* Klinkenberg permeability (kik) can be predicted within a factor of 4.5X (1 standard deviation) using: $\log k_{ik} = 0.282\ \phi_i + 0.18\ RC2 - 5.13$. Artificial neural network analysis, also incorporating the information concerning sedimentary structure as described by rock digit 4 (RC4), provides the capability of predicting k_{ik} within a factor of 3.3X (1 std dev). Analysis is proceeding on routine and in situ capillary pressure, and formation resistivity factor.

TABLE OF CONTENTS

LIST OF TABLES

LIST OF FIGURES

Acronyms

DOE = Department of Energy
k_{ik} = *in situ* Klinkenberg permeability, millidarcies
md = millidarcy, 1 md = 9.87×10^{-4} μm^2
n = number
psi = pound per square inch, 1 psi = 6.89 kPa
ϕ = porosity, percent or fraction depending on context

INTRODUCTION

Objectives - Industry assessment of the regional gas resource, projection of future gas supply, and exploration programs require an understanding of the reservoir properties and accurate tools for formation evaluation of drilled wells. The goal of this project is to provide petrophysical formation evaluation tools related to relative permeability, capillary pressure, electrical properties and algorithm tools for wireline log analysis. Major aspects of the proposed study involve a series of tasks to measure drainage critical gas saturation, capillary pressure, electrical properties and how these change with basic properties such as porosity, permeability, and lithofacies for tight gas sandstones of the Mesaverde Group from six major Tight Gas Sandstone basins (Washakie, Uinta, Piceance, Upper Greater Green River, Sand Wash and Wind River). Critical gas saturation (Sgc) and ambient and *in situ* capillary pressure (Pc) will be performed on 150 rocks selected to represent the range of lithofacies, porosity and permeability in the Mesaverde.

Project Task Overview -

Task 1. Research Management Plan
Task 2. Technology Status Assessment
Task 3. Acquire Data and Materials
- Subtask 3.1. Compile published advanced properties data
- Subtask 3.2. Compile representative lithofacies core and logs from major basins
- Subtask 3.3. Acquire logs from sample wells and digitize

Task 4. Measure Rock Properties
- Subtask 4.1. Measure basic properties (k, ϕ, grain density) and select advanced population
- Subtask 4.2. Measure critical gas saturation
- Subtask 4.3. Measure in situ and routine capillary pressure
- Subtask 4.4. Measure electrical properties
- Subtask 4.5. Measure geologic and petrologic properties
- Subtask 4.6. Perform standard logs analysis

Task 5. Build Database and Web-based Rock Catalog
- Subtask 5.1. Compile published and measured data into Oracle database
- Subtask 5.2. Modify existing web-based software to provide GUI data access

Task 6. Analyze Wireline-log Signature and Analysis Algorithms
- Subtask 6.1. Compare log and core properties
- Subtask 6.2. Evaluate results and determine log-analysis algorithm inputs

Task 7. Simulate Scale-dependence of Relative Permeability
- Subtask 7.1. Construct basic bedform architecture simulation models
- Subtask 7.2. Perform numerical simulation of flow for basic bedform architectures

Task 8. Technology Transfer, Reporting, and Project Management
- Subtask 8.1 Technology Transfer
- Subtask 8.2. Reporting Requirements
- Subtask 8.3. Project Management

EXECUTIVE SUMMARY:

Analysis of the remaining core plugs of the total of approximately 1300 unique sample depths and 700 duplicate core plugs has been proceeding. Arrangements have been made for obtaining final additional samples from industry participants in the next quarter. Analysis of the basic petrophysical properties of the Mesaverde cores measured-to-date indicates that the samples obtained for each basin exhibit approximately the entire porosity and permeability range exhibited by the Mesaverde for all samples analyzed. Grain density for all samples averages 2.654±0.033 g/cc (error of 1 std dev) with grain density distributions differing slightly among basins. Analysis of the permeability data indicates that the Klinkenberg gas slip proportionality constant, b, can be predicted using the relation: $b(atm) = 0.851\ k_{ik}^{-0.341}$. This equation is similar to previously reported equations but extends previous work to lower permeability and significantly increases the population for permeabilities less than 0.01 mD. Using multivariate linear regression analysis the relationship between *in situ* porosity (ϕ_i), the rock characterization size-sorting digit 2 (RC2) and *in situ* Klinkenberg permeability (kik) can be predicted within a factor of 4.5X (1 standard deviation) using: $\log k_{ik} = 0.282\ \phi_i + 0.18\ RC2 - 5.13$. Artificial neural network analysis, also incorporating the information concerning sedimentary structure as described by rock digit 4 (RC4), provides the capability of predicting k_{ik} within a factor of 3.3X (1 std dev). Analysis is proceeding on routine and in situ capillary pressure, and formation resistivity factor.

RESULTS AND DISCUSSION:

TASK 3. ACQUIRE DATA AND MATERIALS

Subtask 3.2. Compile representative lithofacies core and logs from major basins

Figure 1 illustrates the relationship between *in situ* Klinkenberg permeability and calculated *in situ* porosity for all samples measured to date by basin. In situ porosity was calculated using the routine-to-*in situ* correlation presented by Byrnes (2005) where *in situ* porosity is 0.8 porosity units less than routine porosity. The figure illustrates that nearly the complete range in porosity and permeability exhibited by Mesaverde sandstones is present in all basins. Differences in permeability at a given porosity among basins can be primarily attributed to differences in grain size as discussed below. Samples with higher porosity (ϕ>12%) were not sampled in the Wind River Basin or ϕ>16% in the Powder River Basin. Based on examination of wireline logs this absence in the core samples reflects sampling and not absence of this range in porosity within the basins.

Arrangements have been made with several companies for submission of core samples into the program before the sampling phase is closed. These samples will arrive in the last quarter of 2006. Given the present population of samples, no additional samples will be obtained for the project other than these submissions.

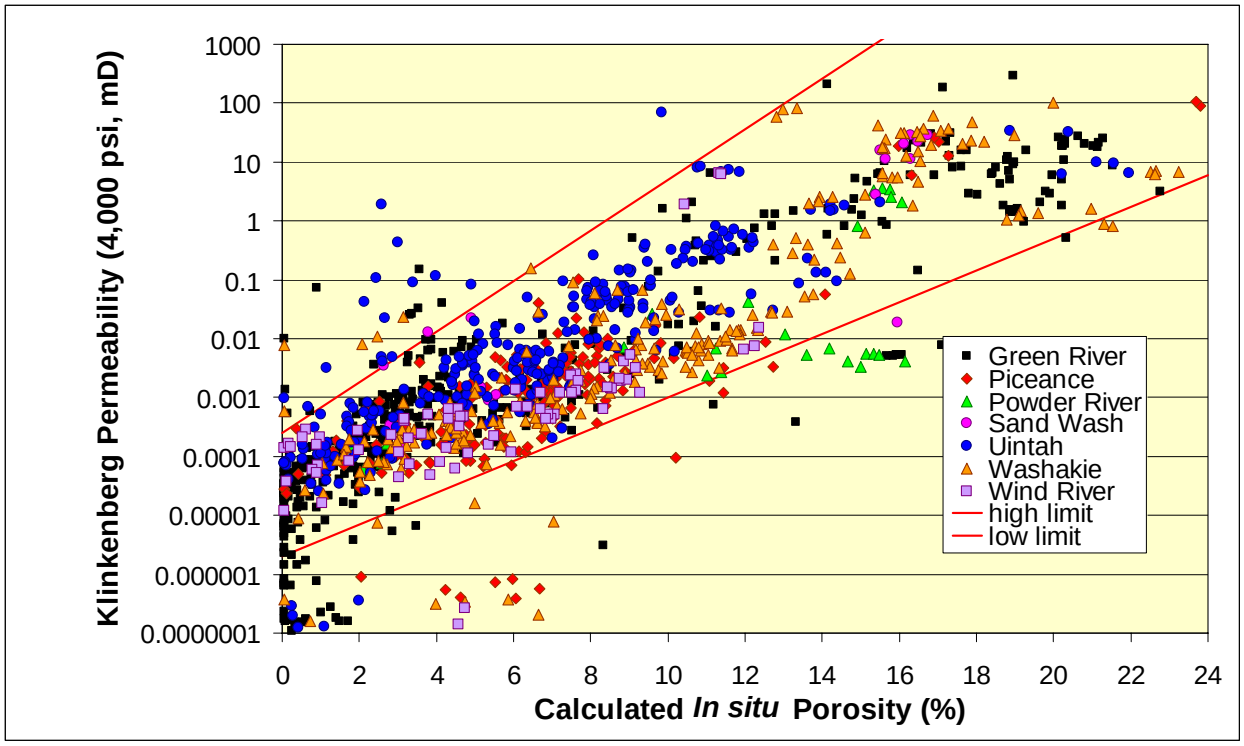

Figure 1. *In situ* Klinkenberg permeability versus calculated *in situ* porosity for all core samples measured to date by basin. Range of porosity and permeability of Mesaverde sandstones is generally exhibited by all basins. Absence of higher porosity samples for Wind River and Powder River samples is interpreted to be due to sampling and not lack of high porosity rocks in these basins.

Subtask 3.3. Acquire logs from sample wells and digitize

Logs have been obtained for many of the wells for which core plugs were obtained. The remaining logs are being obtained.

TASK 4. MEASURE ROCK PROPERTIES

Subtask 4.1. Measure basic properties (k, ϕ, grain density) and select advanced population

Figure 1 illustrated the general permeability-porosity trend for Mesaverde sandstones samples measured to date. Nearly all samples that exhibit permeability greater than the "high" trendline exhibited either; 1) a microfracture, 2) a parting along a shale or carbonaceous lamina, 3) significant lithofacies heterogeneity for some fraction of the core plug parallel to flow (e.g. a high permeability sandstone within less porous lithofacies). Samples exhibiting permeability below the "low" trendline generally exhibited either; 1) churned/bioturbated lithology, 2) cross-bedding with laminae not parallel to flow, 3) extremely fine-grained, or 4) significant clay content.

Grain density distribution for the samples measured to date average 2.654+0.033 g/cc (error bar is 1 standard deviation; Fig. 2). Grain density distribution is skewed slightly to high density reflecting variable concentration of calcite, dolomite, and rare pyrite cement. Grain densities for the wells sampled exhibit a slight difference in distribution between basins (Fig 3, Table 1). It is important to note the small sample population of the Powder, Sand Wash and Wind River Basin samples and these may be biased for conditions in a few wells and intervals.

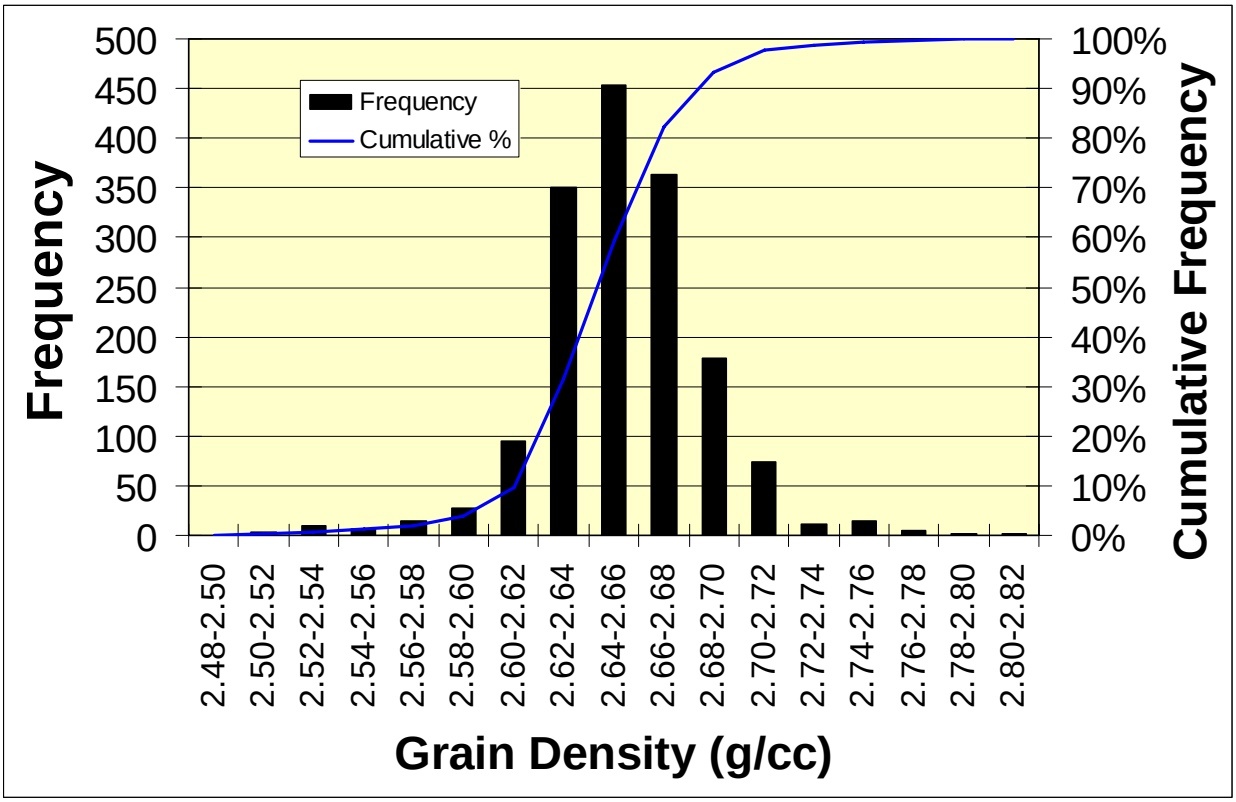

Figure 2. Grain density distribution for all basins and all samples measured to date (n=1619). Distribution is near normal with mean = 2.654+0.033 g/cc. Slight skewness to higher values primarily reflects variable concentration of carbonate cement.

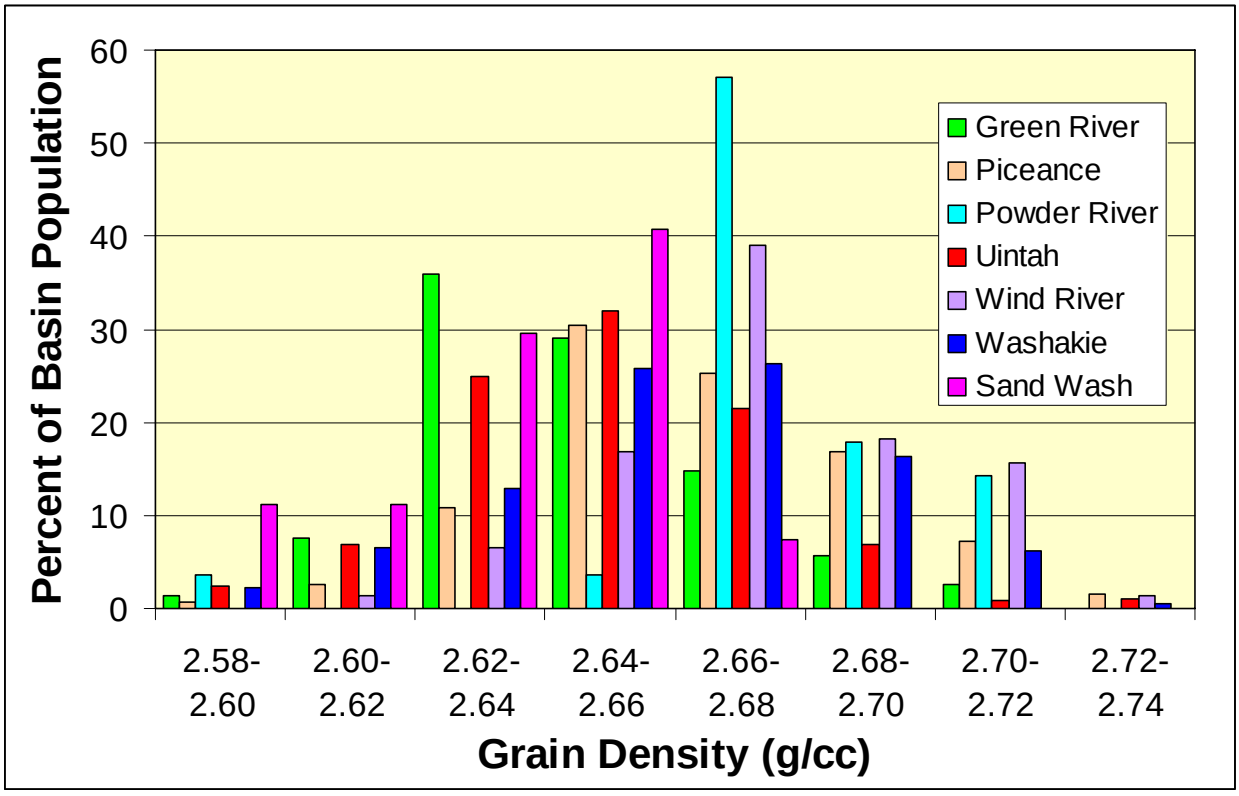

Figure 3. Grain density distribution by basin showing differences between basins as in Table 1.

	All Basins	Green River	Piceance	Powder River	Sand Wash	Uintah	Wind River	Washakie
mean	2.654	2.645	2.663	2.679	2.633	2.646	2.672	2.662
median	2.652	2.641	2.662	2.674	2.639	2.648	2.673	2.661
stdev	0.033	0.028	0.035	0.026	0.020	0.031	0.029	0.034
min	2.505	2.505	2.528	2.599	2.593	2.522	2.515	2.511
max	2.853	2.770	2.801	2.747	2.672	2.770	2.727	2.853
kurtosis	3.323	3.517	3.333	3.928	0.173	3.358	10.378	4.054
skew	0.031	0.353	-0.250	-0.284	-0.568	-0.800	-2.045	0.526
count	1611	488	267	28	27	378	77	373

Table 1. Summary statistics for grain density for samples measured to date by basin.

The porosity distribution of the core samples analyzed to date is skewed to lower porosity (Fig. 4) consistent with general porosity distribution in the Mesaverde sandstone. The large population of cores with porosity of ϕ=0-2% partially reflects a heavy sampling of low porosity intervals in two Green River Basin wells (Fig. 5). At present in situ porosity is being calculated using the equation presented by Byrnes (2001, 2005) where $\phi_{insitu} = \phi_{routine}$-0.8. Future compressibility measurements will further test this relation for the Mesaverde samples in this study.

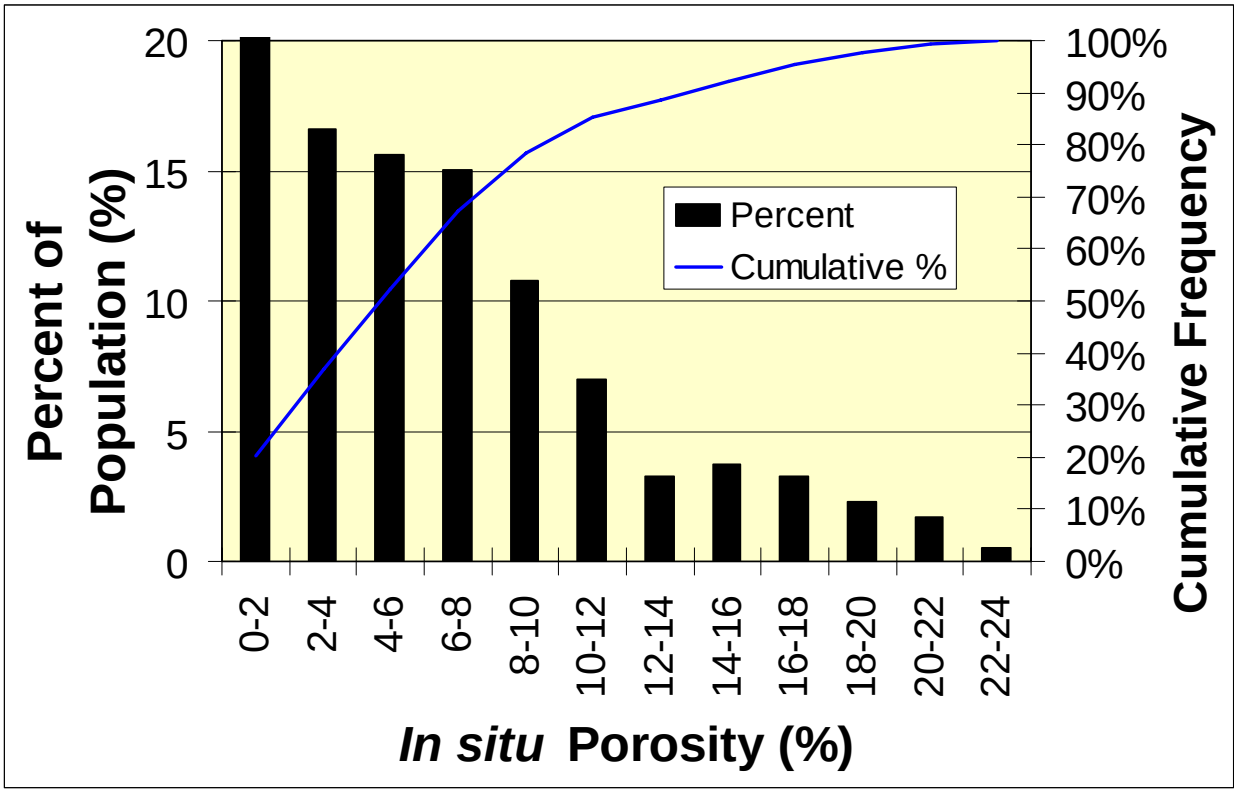

Figure 4. Porosity distribution for all samples measured to date (n = 1619).

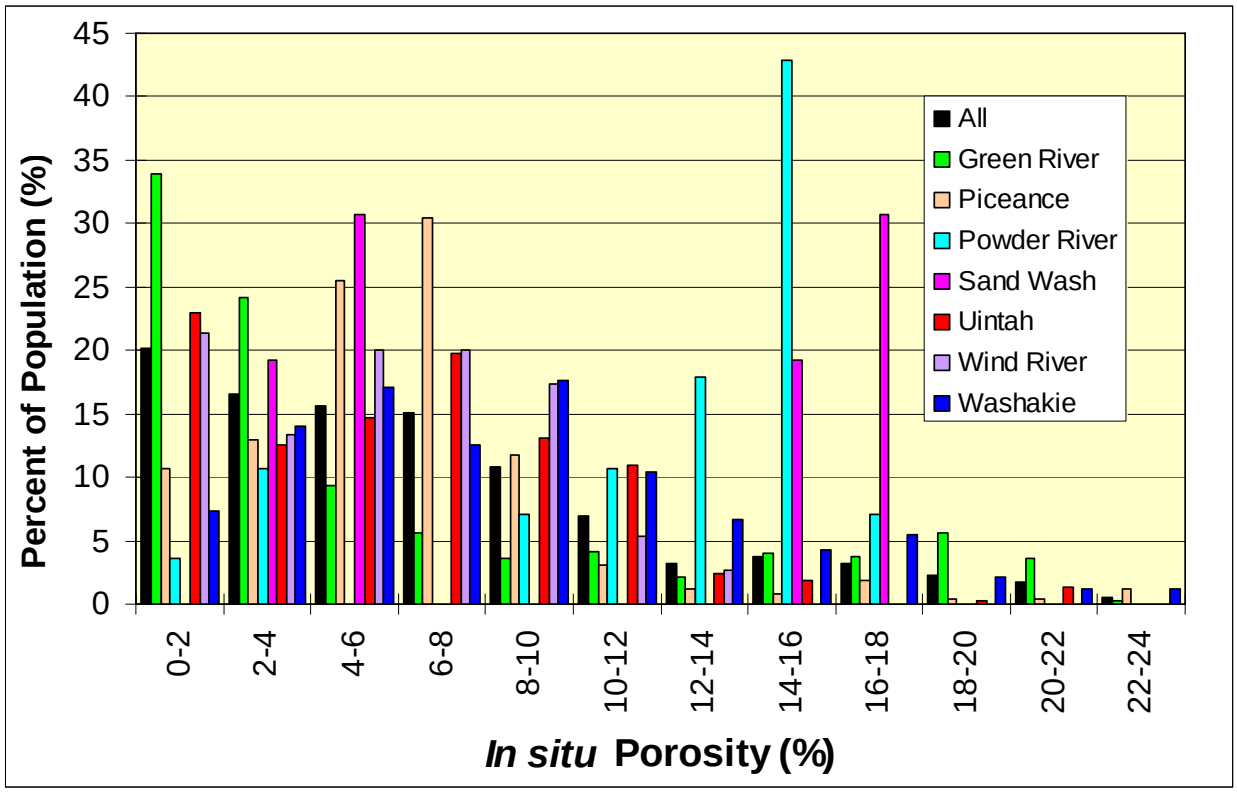

Figure 5. Porosity distribution by basin.

To provide a common reference stress reference frame i*n situ* Klinkenberg permeability has been measured at 4,000 psi net overburden stress and for many at an in situ net effective stress equal in pounds per square inch to half the depth in feet (e.g. a sample from 10,000 feet in depth would have a net effective stress equal to 5,000 psi applied). In situ Klinkenberg permeability was determined by measurement of permeability to nitrogen at two pore pressures and extrapolation of the k vs. 1/P trend to infinite pore pressure to obtain the Klinkenberg permeability at the intercept. The Klinkenberg gas permeability, which is equivalent to single-phase inert liquid or high pressure gas absolute permeability, increases with decreasing pore size. The influence of Klinkenberg gas slippage, which results from greater gas movement due to decreases molecule-molecule interactions at lower pressure, was characterized by Klinkenberg (1954) as:

$$k_{gas} = k_{liquid} (1 + 4cL/r) = k_{liquid} (1 + b/P)$$

where k_{gas} = gas permeability at pore pressure, k_{liquid} is liquid permeability and is equal to the Klinkenberg permeability k_{klink}, c = proportionality constant ($\simeq$ 1), L = mean free path of gas molecule at pore pressure, r = pore radius, b = proportionality constant (=f(c, L, r)), and P = pore pressure (atm). Since b is a function of pore radius distribution it can vary between rock samples. However, general values for b can be estimated from the relation presented by (Heid et al, 1950):

$$b = 0.777\ k_{klink}^{-0.39}$$

and Jones and Owens (1980):

$$b = 0.867\ k_{klink}^{-0.33}$$

Figure 6 shows the Klinkenberg proportionality constant b values measured on core in this study. Reduced major axis analysis predicts a slope and coefficient intermediate between values reported by Jones and Owens (1980) and Heid et al (1950). The b term is expressed in atmospheres. This figure extends the published trend to permeabilities below 0.001 md and significantly supplements the public data for the trend for permeabilities less than 0.01 mD. The variance in b at any given permeability is interpreted to result from several possible conditions including; 1) variance in lithology and corresponding pore throat size and size distribution for the same permeability, 2) heterogeneity of samples resulting in variable b within a sample and resulting averaging of the measured b during measurement, 3) variable b from one end of the sample to the other due to pressure drop across sample, 4) error in one or both gas permeability measurements.

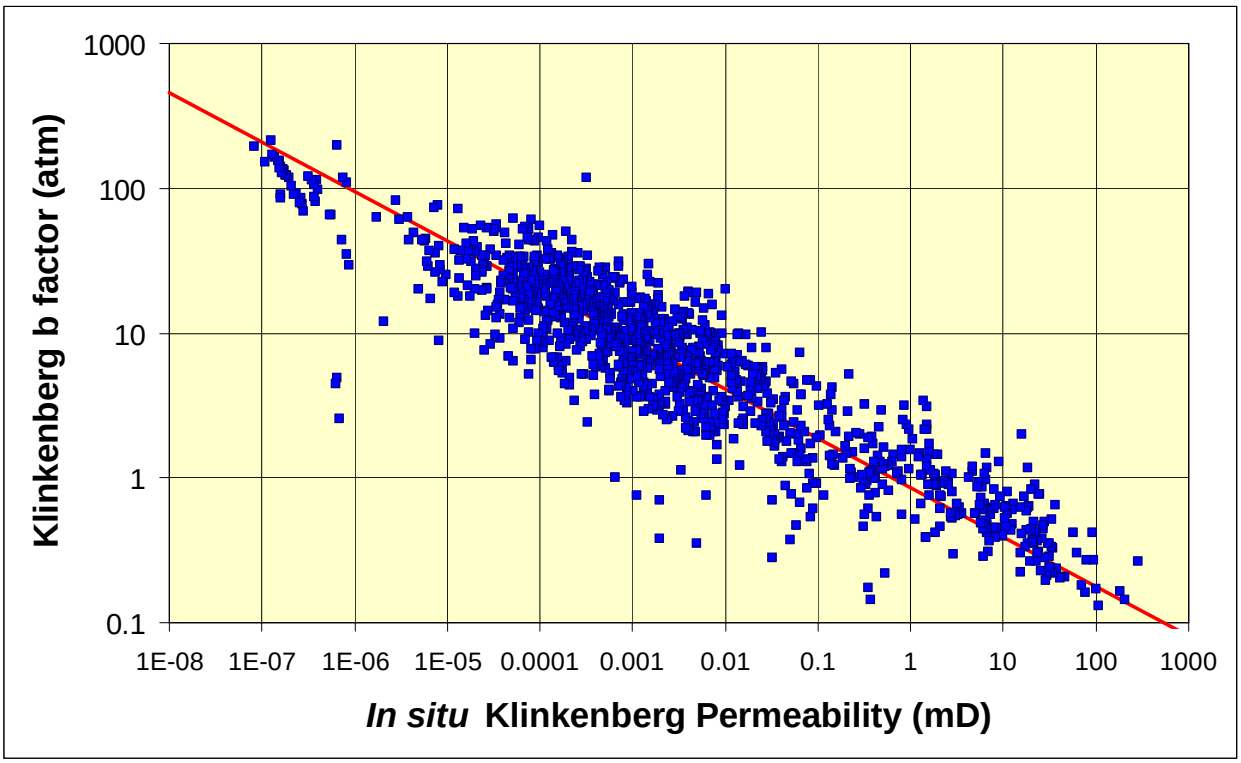

Figure 6. Crossplot of Klinkenberg proportionality constant, b, versus *in situ* Klinkenberg permeability measured at 4,000 psi net effective stress using nitrogen gas. Reduced major axis analysis indicates the correlation can be expressed as $b(atm) = 0.851\ k_{ik}^{-0.341}$, n = 1264.

Permeability for the samples analyzed to date is log-normally distributed (Fig. 7) with 52% of the sample exhibiting in situ Klinkenberg permeability in the range 0.0001-0.01 mD and 18% of the samples exhibiting $k_{ik} < 0.0001$ mD and 30% exhibiting $k_{ik} > 0.01$ mD. The distribution of permeability for samples from different basins is generally similar (Fig. 8) though slight differences in the mean and standard deviation exist. It is important to note that these distributions are for the sample set and may not reflect actually distributions within the basins.

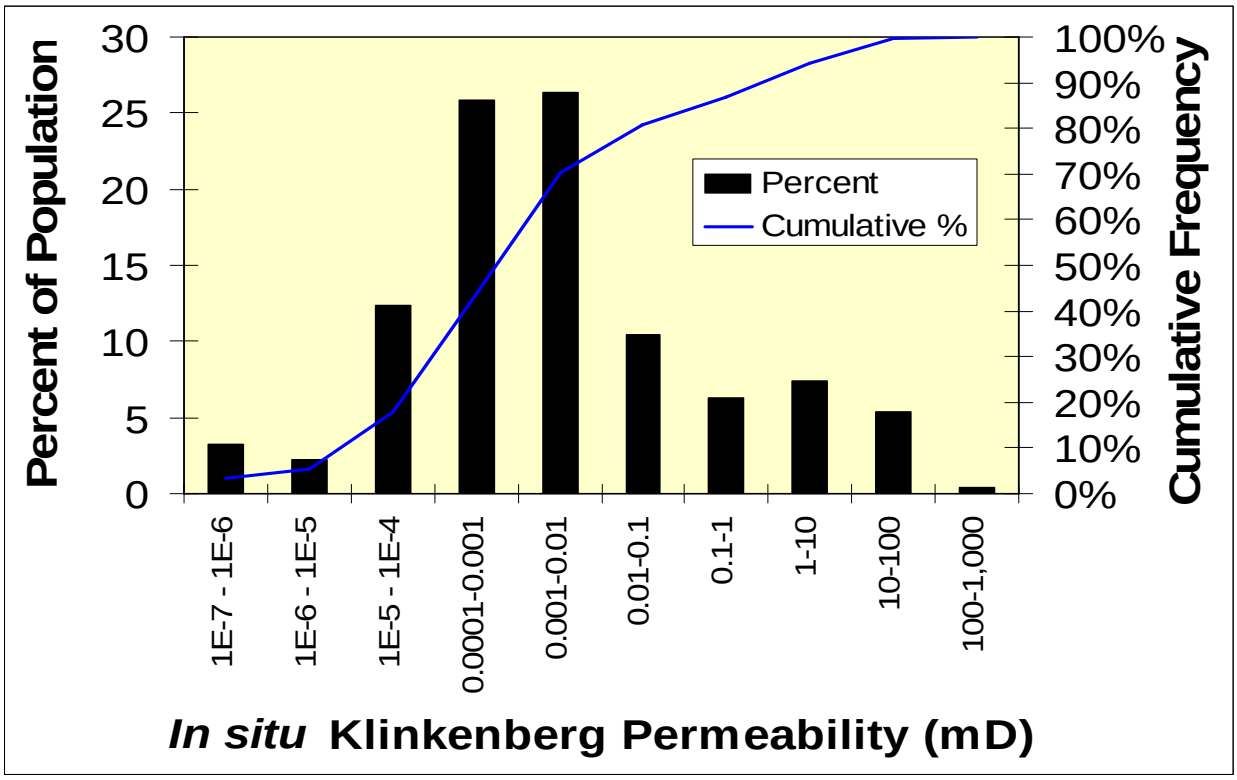

Figure 7. Distribution of *in situ* Klinkenberg permeability measured at 4,000 psi net effective stress for all samples measured to date.

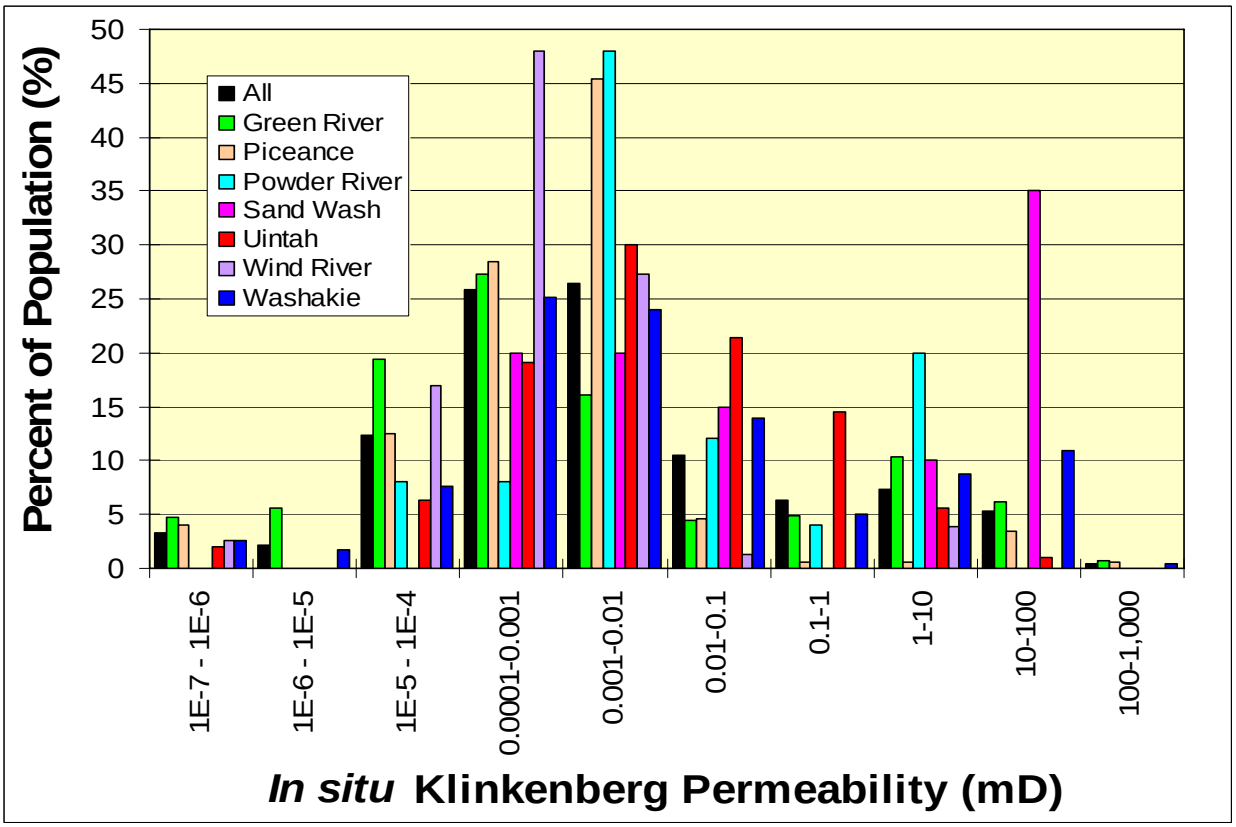

Figure 8. Distribution of *in situ* Klinkenberg permeability measured at 4,000 psi net effective stress by basin.

Figure 9 illustrates the relationship between permeability and porosity parametric with the second rock classification digit which represents size-sorting (see March 2006 quarterly report). Characteristic of most sandstones, permeability at any given porosity increases with increasing grain size and increasing sorting though this relationship is further influenced by sedimentary structure (rock digit 4) and the nature of cementation (rock digit 5). Samples exhibiting permeability greater than the empirically defined high limit generally exhibit an anomalous lithologic property that influences core plug permeability such as microfracturing along fine shale lamination, microfracture, lithologic heterogeneity parallel to bedding with the presence of a high permeability lamina in a core plug dominantly composed of a lower permeability-porosity rock. Conversely, cores exhibiting permeability below the lower limit can exhibit such lithologic properties as churned-bioturbated texture, cross-bedding with fine-grained or shaly bed boundaries that are sub-parallel or perpendicular to flow and act as restrictions to flow, or high clay content. Permeability in low porosity samples and particularly below approximately 1% (vertical red line) is generally a complex function of final pore architecture after cementation and is only weakly correlated with original grain size. The estimated range in permeability at any given porosity increases with porosity and can be as great as four orders of magnitude for $\phi >$ 12% but decreases to approximately 20X near ϕ=0%. Though in unconsolidated grain packs the influence of size and sorting can be quantified, in consolidated porous media the influence of these variables and particularly the influence of sedimentary structure can be non-linear and non-continuous. For example coarse grain size results in high permeability but if the sand was deposited in a trough cross-bedded structure and there is some orientation of bedding in the core that is not parallel to flow then the permeability can be significantly reduced. The rock classification system used works to both quantify and make continuous these parameters but has limits.

Excluding samples exhibiting permeability outside the limits shown in Figure 9 the relationship between the porosity and lithologic variables and permeability was explored. Multivariate linear regression analysis provides a predictive relationship:

$$\log k_{ik} = 0.282\ \phi_i + 0.18\ RC2 - 5.13$$

where k_{ik} is the in situ Klinkenberg permeability at 4,000 psi net confining stress (mD), ϕ_i is the insitu porosity (%) and RC2 is the second digit of the rock classification representing size-sorting. Standard error of prediction for this equation is a factor of 4.5X (1 standard deviation). Non-linear multivariate regression analysis does not significantly improve predictive capability. The simplest non-linear relation that is not a polynomial that is adjusted to fit the k_{ik}-ϕ_i surface is:

$$\log k_{ik} = 0.034\ \phi_i^2 - 0.00109\ \phi_i^3 + 0.0032\ RC2 - 4.13$$

which exhibits a standard error of prediction of 4.1X (1 std dev).

Because of the non-linear nature of the influence of the independent variable an artificial neural network (ANN) approach was also examined. A single hidden layer, 10 node network was used where the output from the hidden layer was a sigmoidal function (1/1+exp(-x)) of the hidden-layer output. Table 2 shows the ANN parameters. The ANN, using *in situ* porosity (Phii), RC2 and RC4 provides prediction of k_{ik} with a standard error of prediction of 3.3X (1 std dev, Fig. 10). These relationships will be explored further when collection of all basic data and rock typing is complete.

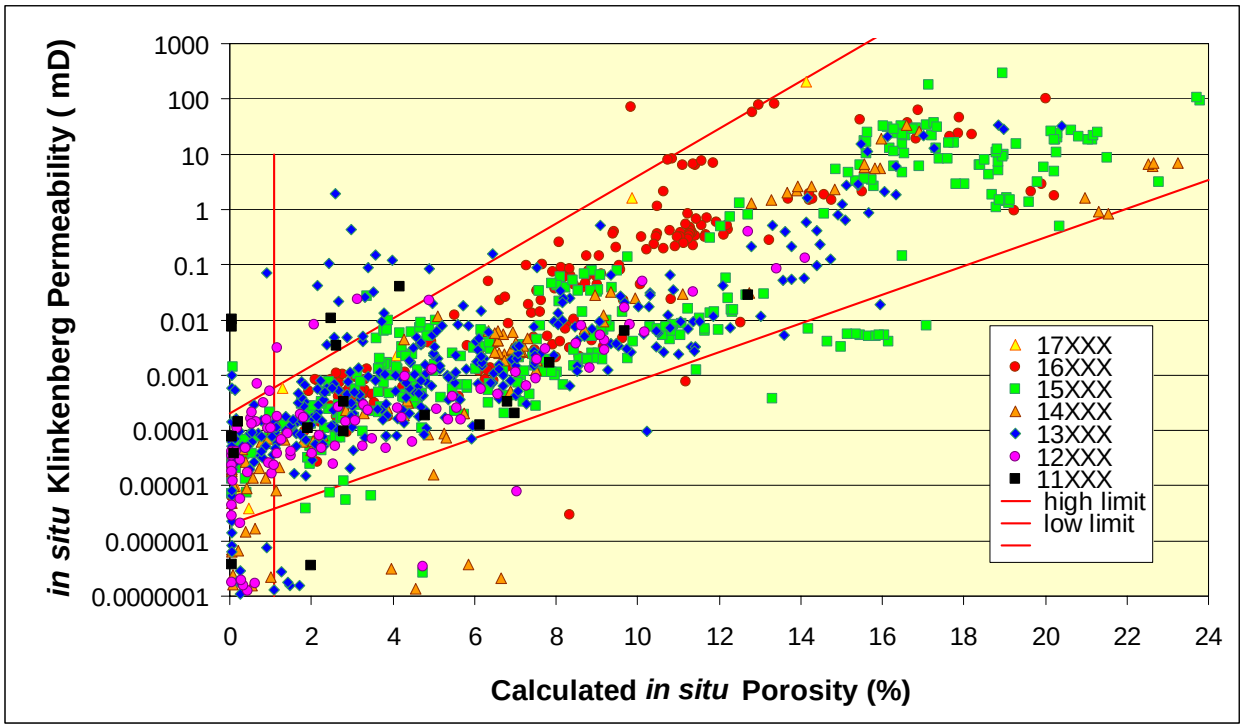

Figure 9. Crossplot of i*n situ* Klinkenberg permeability (k_{ik}, mD, measured at 4,000 psi net effective stress) versus calculated *in situ* porosity ($f_{routine}$-0.8) for all core samples measured to date by second rock type digit representing size-sorting. The high limit generally defines the upper range for medium-coarse grained rocks. The lower limit generally represents the limit for lower very fine-grained to siltstone rocks. Permeability in samples with porosity below approximately 1% (vertical red line) is generally a complex function of final pore architecture after cementation and is only weakly correlated with original grain size. Samples with permeability higher and lower than the high and low limits respectively generally exhibit anomalous lithologic properties such as shale parting fracture, churned-bioturbated texture, lithologic heterogeneity, etc.

hidden layer: 1					
Hidden layer nodes: 10					
	Mean>	8.239	4.280	6.294	hidden layer-
	Std Dev>	5.260	1.335	2.527	to-output
	Input-to-hidden layer weights				weights
Node	Constant	Phii	RC2	RC4	
Constant					-0.388
1	-0.760	2.946	-2.027	-6.438	-0.885
2	-2.155	4.637	1.279	0.895	2.323
3	-4.999	7.901	0.957	3.167	-2.583
4	-1.484	-0.307	-1.695	6.175	-0.154
5	-4.597	4.582	1.568	0.730	4.022
6	-2.609	0.320	-2.201	-2.257	-2.495
7	-1.765	-1.843	-1.122	0.145	-3.859
8	2.839	-3.146	-9.237	0.264	0.789
9	-1.566	1.029	-1.588	-3.390	2.400
10	2.951	0.778	3.316	0.179	-2.136

Table 2. Artificial neural network parameters for kik prediction using ϕ_i, RC2 and RC4 as input variables. ANN utilized was a single hidden layer with 10 nodes and sigmoidal base function.

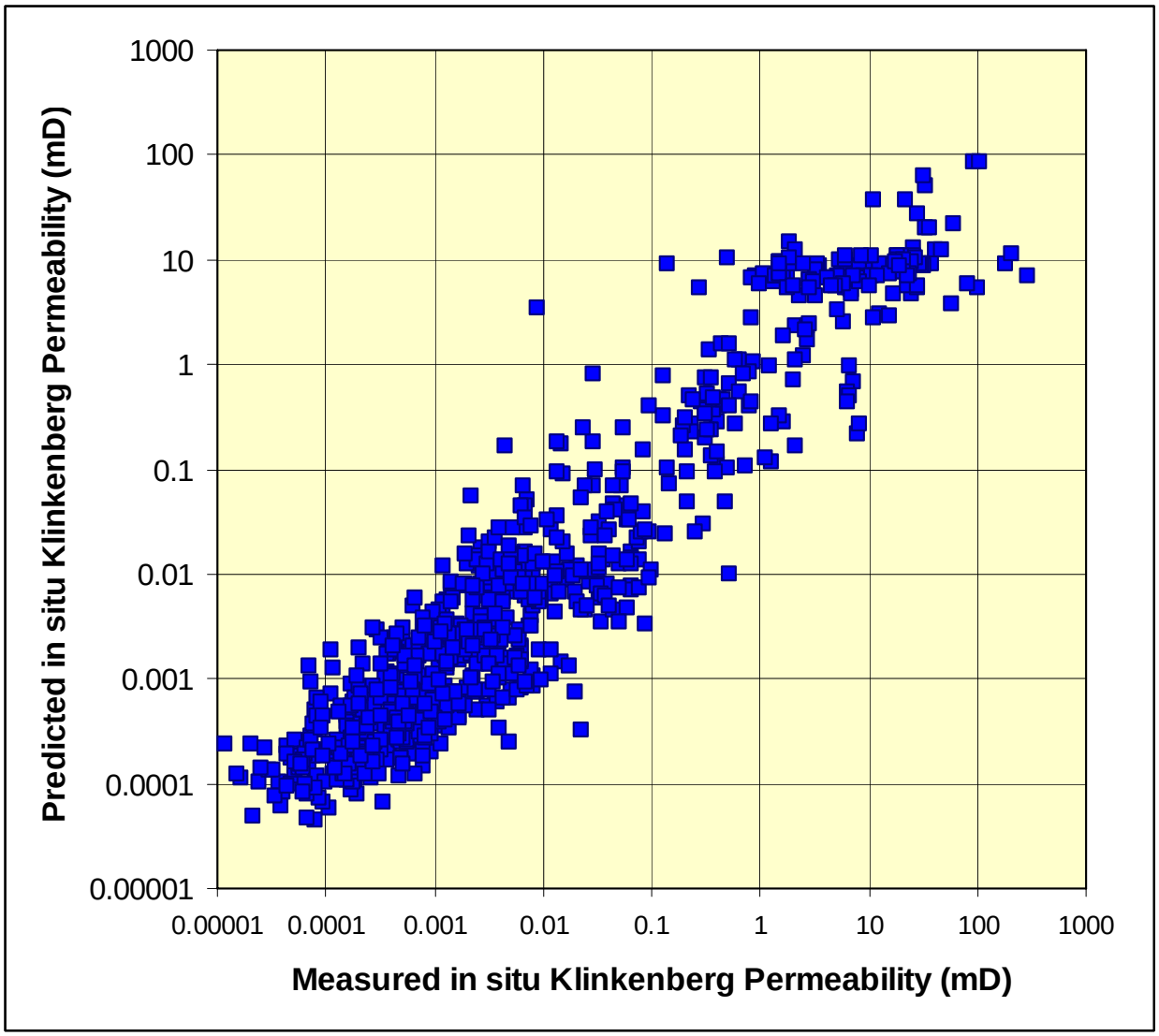

Figure 10. Crossplot of measured versus predicted *in situ* Klinkenberg permeability using artificial neural network with parameters shown in Table 2. Correlation standard error is 3.5X.

Subtask 4.3. Measure *in situ* and routine capillary pressure
Capillary pressure analysis is continuing on selected samples.

CONCLUSIONS

Cores continue to be contributed by industry participants though this will begin to be curtailed in the next quarter due to sample number and scheduling constraints. Basic and advanced properties measurements are preceding smoothly and only slightly behind the timetable presented in the Management Plan. The minor delay is the result of analysis of nearly four times the number of samples originally proposed. Analysis is being performed within the approved budget. Although the Mesaverde exhibits a wide range of lithologies, porosity, and permeability, for the same lithofacies and porosity rocks in all basins are exhibiting similar properties. This will be useful for widespread application of relations developed in the study.